# The ATLAS Liquid Argon Forward Calorimeter Electrode Uniformity

G.Belanger, K.Coley, T.Embry, M.Khakzad, P.Krieger, R.Orr, E.Neuheimer, H.Mes, G.Oakham, J.Rutherfoord*, A.Savine, L.Shaver, M.Starr, V.Strickland, K.Vincent

10 September 2005

The mechanical precision of the electrode gaps contributes to the uniformity of response of a liquid argon calorimeter. The electrode capacitance is a sensitive measure of the gap. The capacitance of every electrode in every ATLAS Forward Calorimeter module has been measured giving an rms deviation ranging from 0.8% to 1.7% depending on the module. In concert with the measurements, we have also calculated the capacitance using measurements of the electrode dimensions. The calculated and measured electrode capacitances show good agreement.

The ATLAS detector at the Large Hadron Collider (LHC) will measure the products of the collisions of two protons at the highest energies yet achieved. Some of these products are expected to be new and different from anything we've seen before. To find the occasional, interesting event mixed with a huge number of more ordinary events requires superb instrumentation.

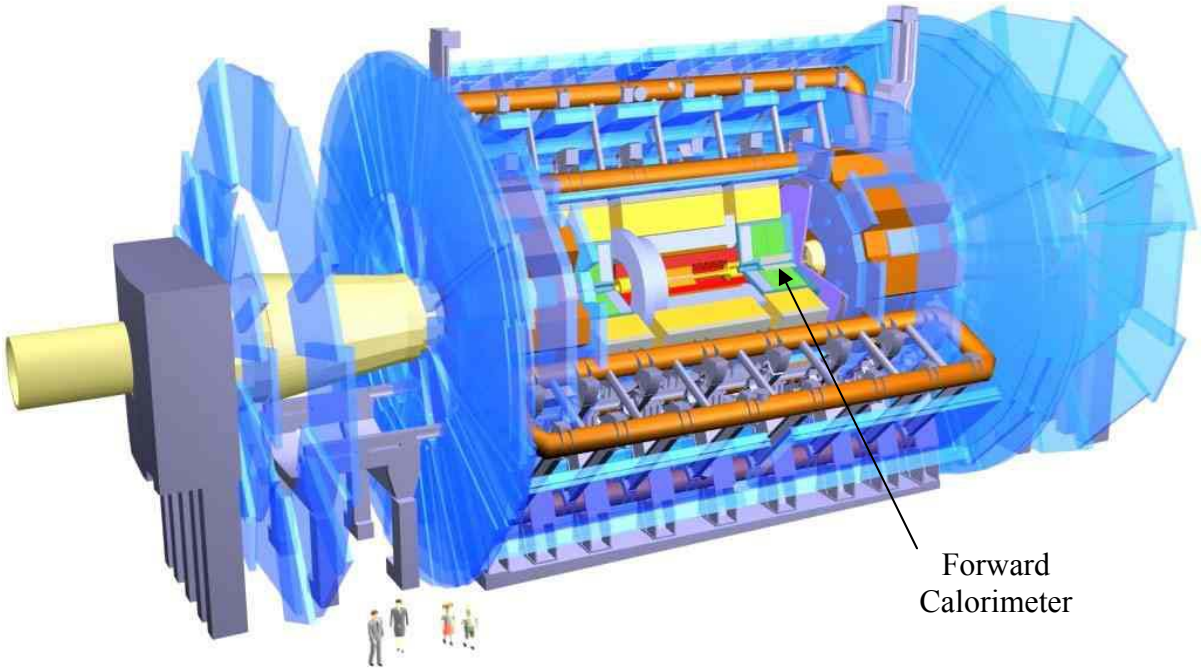


Figure 1. Drawing of the ATLAS Detector with parts cut away to show some of the inner components. One of the two Forward Calorimeters (white) can be seen inside the HEC (green).

The ATLAS Calorimeter System measures the energy and position of most of the product particles from the collisions. The Forward Calorimeters are located closest to the beam line, one on each side of the Interaction Point. One is shown in Figure 1. Because the radiation environment is most severe at small angles to the beams, no other detector elements overlap this angular region.

Each of the two Forward Calorimeters (named FCalA and FCalC) consists of three modules, one behind the other, designated FCal1, FCal2, and FCal3 respectively. Each module is of similar but not identical construction. The module closest to the Interaction Point is made of copper while the succeeding two are made mostly of tungsten.

All of the electromagnetic calorimeters in ATLAS and some of the hadronic calorimeters are ionization sampling detectors with liquid argon as the sensitive medium. The Forward Calorimeters are of this technology. The liquid argon electrodes (the ionization chambers) for the forward calorimeters have a different geometry from the other liquid argon calorimeters. Here the liquid argon gap is a cylindrical shell bounded at the inner radius by a rod and at the outer radius by a tube. The rod is held in place inside the tube by a helically-wound insulating fiber. Over the length of the electrode, about 450 mm, there are about 10 turns (windings) of the fiber. Figure 2 shows this geometry. Another distinctive feature of these electrodes is that the gap is quite small. For the Forward Calorimeter the gaps are about 0.250, 0.375, and 0.500 mm for the three modules (in order of distance from the Interaction Point) compared to about 2 mm for many other liquid argon calorimeters. The electrode rod is held at positive potential and the tube at ground potential so that the electric field in the gap averages about 1 kV/mm.

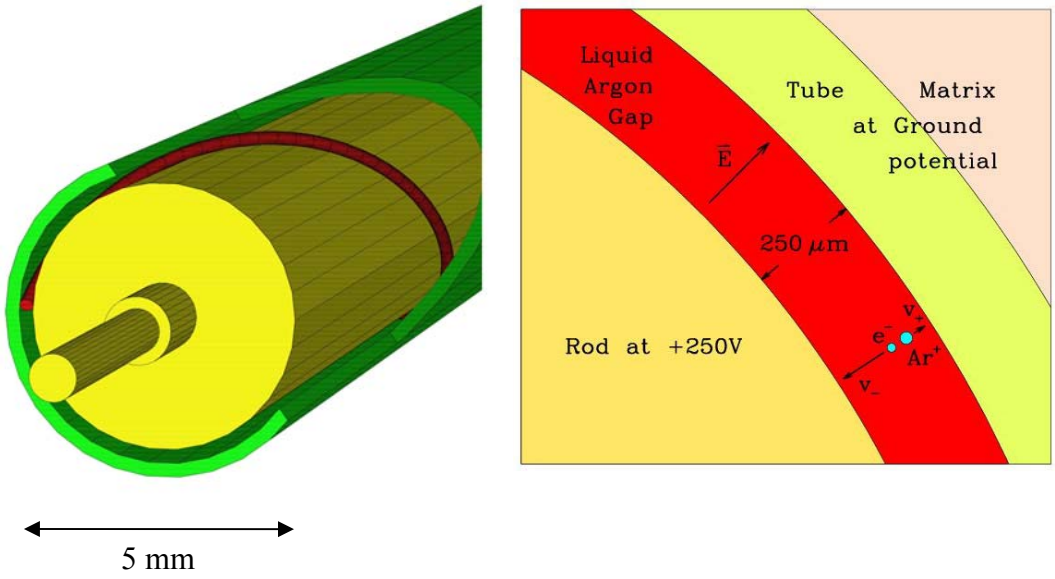


Figure 2. At the left is a drawing of one end of an FCal "tube" electrode showing the tube (with a part cut away), rod, helically wound insulating PEEK fiber, and readout pin. On the right is a close-up cross section of an FCal1 electrode showing the liquid argon gap, the tube, and the rod. Each electrode is embedded in a matrix.

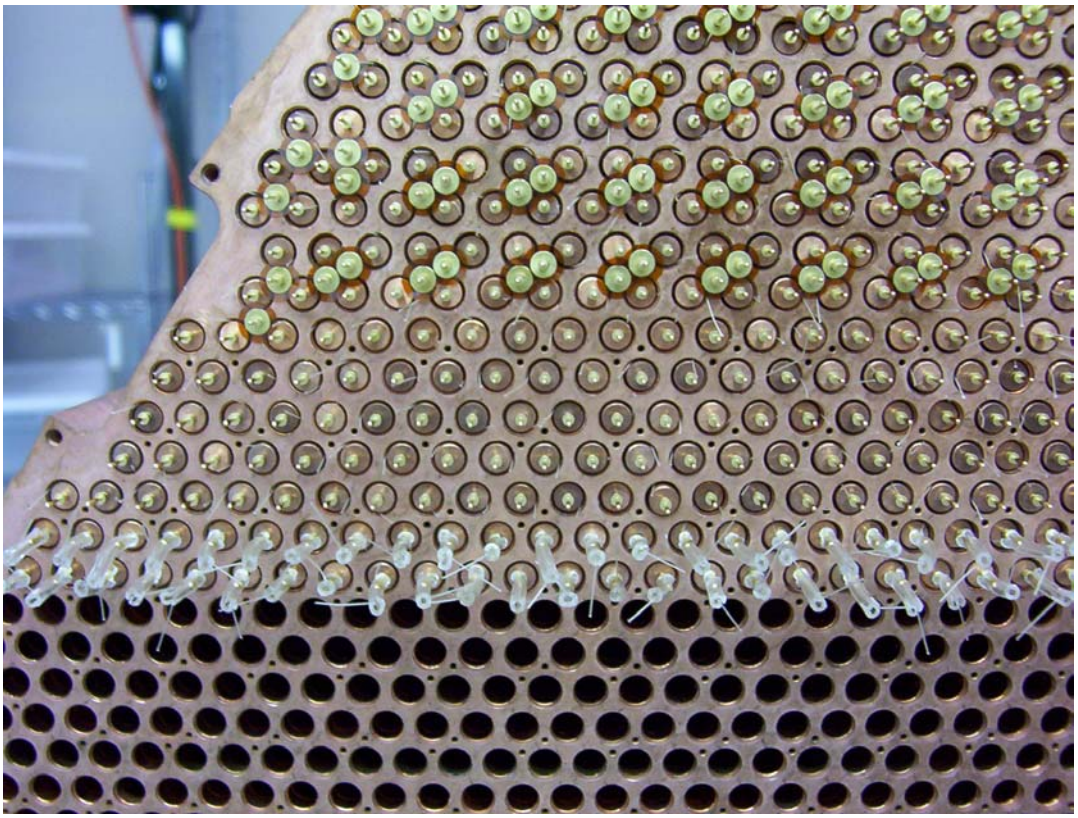

Figure 3. This photograph of a section of an FCal1 module was taken during the construction phase as the electrode rods were being inserted into the tubes. The tubes were already embedded in the copper matrix. At the time of this photo, the upper rows were completed and the intermediate rows were in various stages of processing. The ends of the insulating fibers are visible. Tygon tubing was used to hold the fibers in place during rod insertion and then removed. This view shows the side of the module facing the Interaction Point.

Of order 10,000 such electrodes are inserted into the module absorber matrix in a regular hexagonal array as can be seen in the photograph in Figure 3. Particles from the Interaction Point which hit the calorimeter produce a shower of secondary particles. The charged secondaries crossing the liquid argon gaps ionize the argon atoms. The resulting electrons drift to the rod, producing an electrical pulse. The positive argon ions drift much more slowly to the tube.

The axis of each electrode is parallel to the nominal beam line of the LHC so that particles from the interactions impinge on the calorimeter at a shallow angle to the electrode axis. In order that the size of the electrical signal from the Forward Calorimeter is insensitive to the position of the particle, it is important that each electrode is as identical as possible to all the others in a given module. The uniformity of the electrodes is the subject of this report.

The dimensions of the electrode elements are summarized in Table 1. The liquid argon "Gap" is the critical parameter for the electrical signal. Detailed metrology for FCal1 electrode elements predicted the rms gap width variation to be about 1% [1]. Similar results were obtained for the other modules [2].

To confirm this prediction the FCal community performed detailed measurements of the electrode capacitance for every electrode in every module. This was done in the clean room at CERN with the modules on their pedestals. Thus the dielectric of the gap was air rather than liquid argon.

| | FCal1 | FCal2C | FCal2A | FCal3Chin | FCal3Russ | FCal3Ave |
|---|---|---|---|---|---|---|
| Tube Length | 445.0N | 444.35N | 444.35N | 444.3 | 444.3 | 444.3 |
| Tube OD | 5.753 | 6.185 | 6.165 | 7.01 | 7.01 | 7.01 |
| Tube Wall Thickness | 0.253 | 0.258 | 0.234 | 0.250N | 0.250N | 0.250N |
| Tube ID | 5.250 | 5.669 | 5.697 | 6.51 | 6.51 | 6.51 |
| Rod Length | 445.2 | 443.48 | 443.48 | 443.38 | 443.46 | 443.4 |
| Rod OD | 4.712 | 4.93 | 4.93 | 5.50 | 5.49 | 5.495 |
| Gap (calc) | 0.269 | 0.369 | 0.383 | 0.4883 | 0.4933 | 0.491 |
| PEEK fiber OD | 0.250N | 0.350N | 0.350N | 0.467 | 0.484 | 0.467 |

Table 1. Physical dimensions of the electrode components. Units are mm. N means "nominal", i.e. no measurement was made.

A test station was put together around a Stanford Research Systems Model SR720 LCR Meter. Special probes were constructed to minimize the probe capacitance and the dependence of the probe capacitance on the way the probes were routed from the meter to the electrodes. The LCR meter was allowed to warm up for at least two hours before routine measurements were taken. All measurements were taken at a meter frequency of 100 kHz.

Electrodes were measured in order, starting at the top row and progressing down the module. One electrode, the reference electrode, was measured repeatedly to help keep track of any drifts. Also periodically, the probes were connected to two pins, spaced the same as a signal electrode pin and ground pin on the module, but with no device connected across the pins. This was meant to be a "zero" of capacitance which was called the "blank". A standard capacitor was also measured repeatedly and occasionally five secondary standard capacitors, spanning the range of capacitance of the electrodes, were measured.

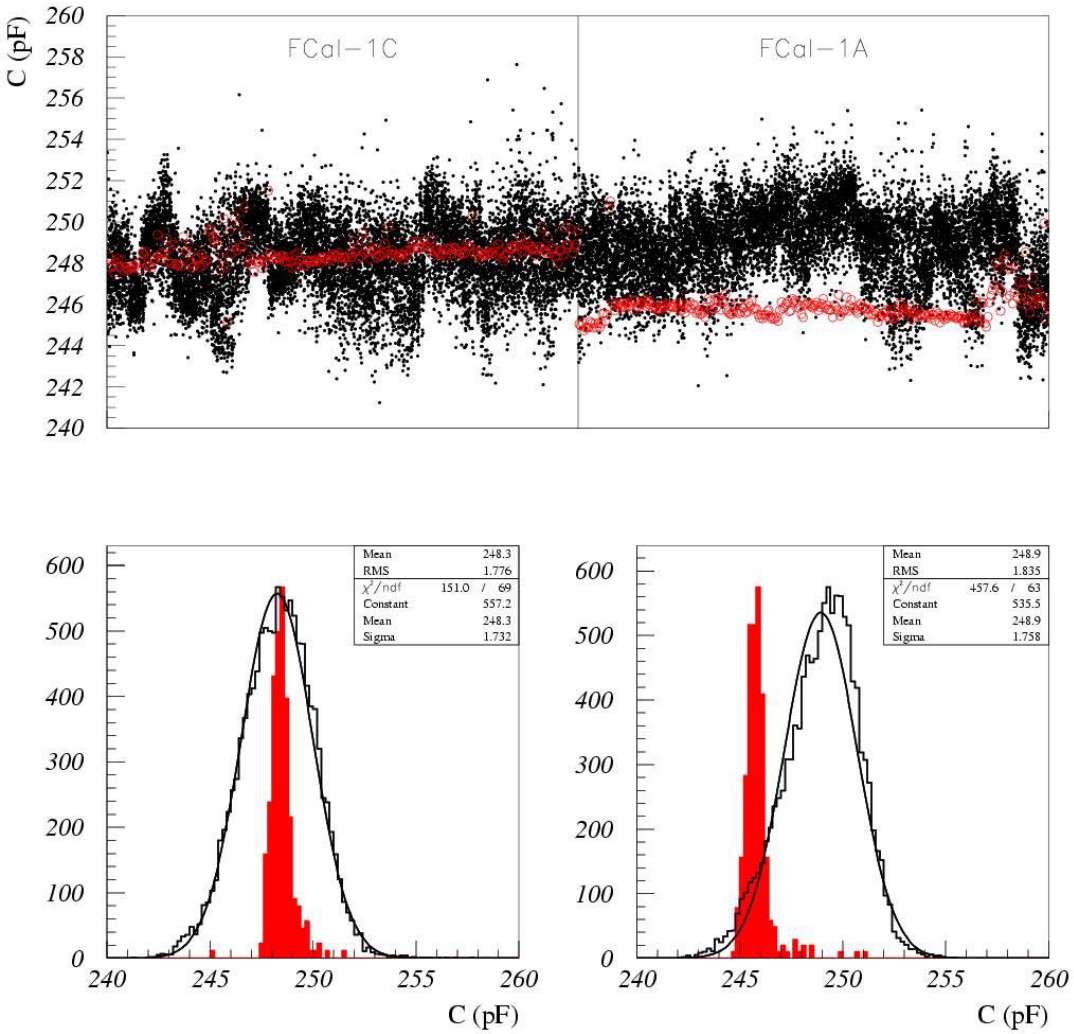


Figure 4. Summary of measurements of the 12,260 FCal1C electrodes and the reference electrode (red) after subtraction of the "blank" capacitor but without further corrections.

| | Calculated Capacitance | Measured Capacitance Before Probe Correction | After |
|---|---|---|---|
| FCal1C Electrodes | 234.5 | 248.3(1.8) | 235.8(1.8) |
| FCal1A Electrodes | 234.5 | 248.9(1.8) | 236.4(1.8) |
| FCal2C Electrodes | 182.4 | 190.0(2.4) | 179.5(2.4) |
| FCal2A Electrodes | 176.7 | 178.5(3.0) | 174.8(3.0) |
| FCal3C Electrodes | 152.0 | 158.1(1.8) | 149.2(1.8) |
| FCal3A Electrodes | 152.0 | 154.5(1.7) | 150.8(1.7) |

Table 2. Summary of calculated and measured FCal electrode capacitances. Units are picoFarads. Numbers in parentheses are rms measurement errors.

The LCR Meter was interfaced via GPIB to a PC running LabVIEW. The program used a data base of the geometry of the modules and kept track of 1) which electrodes had been measured, 2) when the "blank" should be measured, 3) when the reference electrode should be measured, and 4) when the standard capacitor should be measured. It also recorded all the data along with the name of the operator, the date and time of day, and the mode of operation, usually "automatic" where the next electrode was specifiedby the program. The FCal1C, FCal2C, FCal3C, and FCal1A modules were all measured with this setup. The FCal2A and FCal3A modules were measured with an almost identical setup.

Capacitance measurements of the FCal1 electrodes are summarized in Figure 4. The only correction applied at this point is to subtract the "blank". The average over the 12,260 electrodes in each module appears in Table 2, along with the results from the other four modules, in the column labeled "Before Probe Correction".

The rms of the capacitance measurements for FCal1 is about 0.8%, consistent with the metrology noted above. For FCal2 the rms is about 1.5% and for FCal3 about 1.2%. This data suggests that the variation of the gap width of the electrodes is significantly smaller than the constant term in the energy resolution. Capacitance measurements of the one reference electrode, measured periodically to check for drift, had an rms of about 0.15% after rejection of a few outliers. So drift or other instrumental effects are likely a small contribution to the electrode rms values. The rms capacitance measurement of the 400 pF standard capacitor was about 0.02% (about 0.1 pF) and the rms of the "blank" was about 0.06 pF.

When the capacitance measurement test station was developed at Arizona, trials with the standard capacitors all yielded results very close to the nominal. But in the North Area clean room at CERN the values were of order 5% higher. A linear fit to the standard capacitor data also showed a small offset at zero. The newer test station used to measure FCal2A and FCal3A required no scale correction but showed a small offset at zero. These zero offsets are after subtracting the "blank". Swapping the probe cables showed that the scale and offset were properties of the probes and not the LCR meters. The capacitance measurements were corrected for these probe effects and are labeled "After Probe Correction" in Table 2.

Can we understand the absolute values of the measured electrode capacitance in terms of the metrology? Ignoring the insulating PEEK fiber, the end effects, and assuming the rod is coaxial with the tube, it is straightforward to calculate the capacitance. The permittivity of vacuum is 8.8542E-15 F/mm, the dielectric constant of dry air is about 1.0006. For relative humidity of about 60% at 20 C, as at CERN, the water vapor in the air is about 10 g/m^3. With water of dielectric constant about 80, humid air increases the dielectric constant to about 1.0014. So we used the permittivity of humid air of about 8.867E-15 F/mm. These results are shown in Table 3 in the column labeled "Simple".

To calculate the effect of the insulating fiber requires numerical simulation. For this we found finite-element freeware on the web by Field Precision called TriComp 5.0. (See

www.fieldp.com.) This 2-D package set will establish the mesh for problems which have some symmetry allowing to eliminate the third dimension. With the mesh, another package of the set calculates the electric field and the energy (or energy per unit length along the third uniform dimension) in that electric field. In the case of the fiber, the approximation is made that the electrode is infinitely long and that the fiber does not wind helically around the rod but is parallel to the tube and rod axes. As an experimental test of this approximation, we varied the number of turns from 3 to 10. No difference in capacitance could be measured [3]. This was expected because the difference in length of the helically wound fiber of variable pitch is negligible due to the very small pitch angle of the fiber to the rod/tube axis.

For the PEEK fiber a dielectric constant of 3.3 was used [4]. Rather than calculate the capacitance of the electrode with the fiber we, instead, determined the change in capacitance with and without the fiber. We started by simulating just one quadrant of the electrode cross section and used appropriate boundary conditions. The program gave the energy in the electric field per unit length of the electrode. To get the capacitance we multiplied the energy linear density by the length of the electrode and then used the expression for the energy in terms of the capacitance and potential across the electrodes. While all expressions scale properly so that the potential was immaterial, we nevertheless chose the nominal potentials of 250, 375, and 500 V for the FCal1, 2, and 3 electrodes in these calculations. The energies quoted in later tables reflect this choice.

When simulating a quadrant of the electrode cross section, a practical mesh was too coarse to adequately represent the fiber cross section. So we employed a feature of the software to constrain the potential on the boundary of a smaller region to that found with the coarse mesh. Then the potential within this smaller region was found using a fine mesh as shown in Figure 5. Table 4 summarizes all the data from these fiber simulations. The "coarse" and "fine" refer to the two meshes described above. The fine-mesh capacitance changes are carried over to Table 3. In several cases the number in Table 3 is an interpolation of data in Table 4.

| | Simple (pF) | + PEEK (pF) | + end (pF) | Total (pF) |
|---|---|---|---|---|
| FCal1 | 229.4 | 4.7 | 0.4 | 234.5 |
| FCal2C | 177.3 | 5.0 | 0.4 | 182.7 |
| FCal2A | 171.3 | 5.0 | 0.4 | 176.7 |
| FCal3Chin | 146.5 | 5.9 | 0.4 | 152.8 |
| FCal3Russ | 145.0 | 5.9 | 0.4 | 151.3 |
| FCal3Ave | 145.7 | 5.9 | 0.4 | 152.0 |

Table 3. Summary of the capacitance calculations. Units are picoFarads.

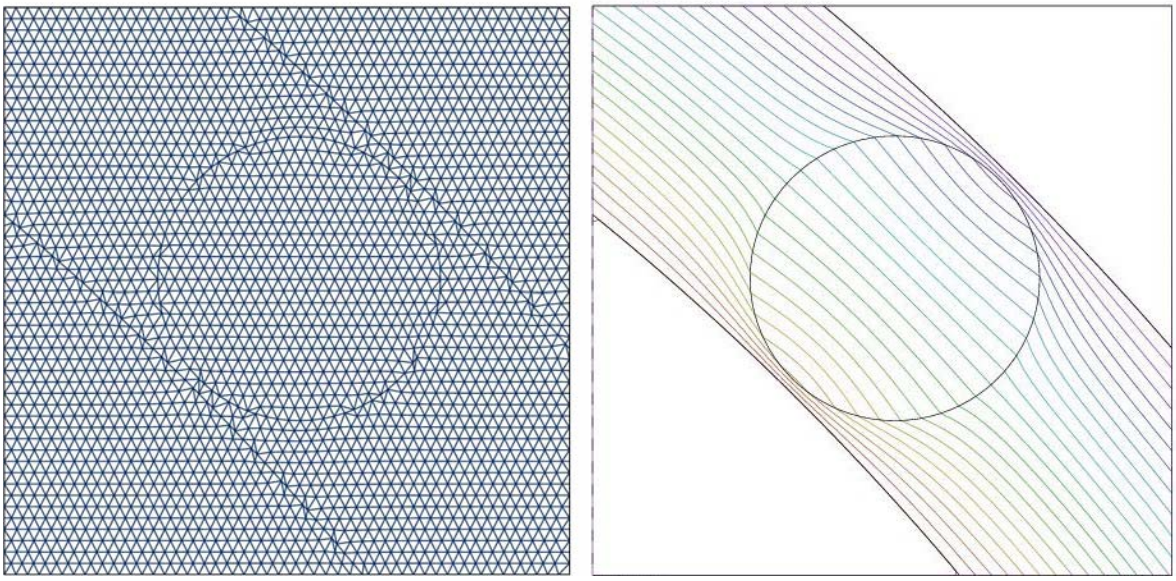

Figure 5. Mesh (left) and equipotential lines (right) for a small section of the FCal1 gap with PEEK fiber.

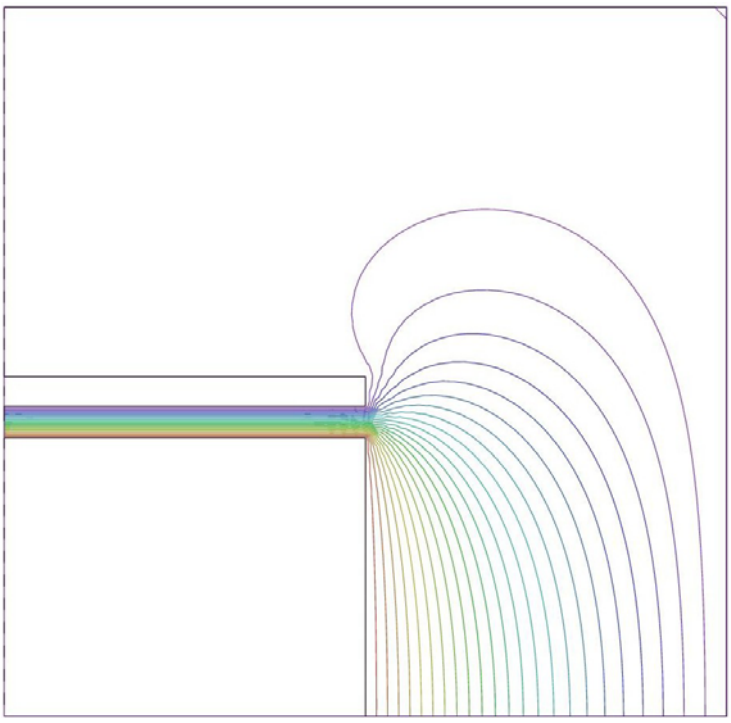

Figure 6. Equipotential lines representing the fringe field at one end of the tube electrode. This is a cross-section of the electrode with the electrode axis along the bottom of the bounding square. Cross sections of the end of the tube and rod are shown in outline.

Also shown in Table 4 is the dependence of the capacitance change on the gap width and the fiber diameter.

| File | Fiber diameter (mm) | Geometry | gap (mm) | Energy Density (J/m) | Change in Capacitance (pF) |
|---|---|---|---|---|---|
| tube1_elec | none | coarse | | 4.027E-06 | |
| tube1_elec_peek | 0.25 | coarse | | 4.490E-06 | 6.60 |
| tube1_elec_f | none | fine | | 5.912E-07 | |
| tube1_elec_peek_f | 0.25 | fine | | 9.214E-07 | 4.70 |
| | | | | | |
| tube2_elec | none | coarse | 0.350 | 7.366E-06 | |
| tube2_elec1 | none | coarse | 0.375 | 6.906E-06 | |
| tube2_elec_peek | 0.35 | coarse | 0.350 | 8.456E-06 | 6.87 |
| tube2_elec_peek1 | 0.35 | coarse | 0.375 | 7.833E-06 | 5.85 |
| tube2_elec_f | none | fine | 0.350 | 1.316E-06 | |
| tube2_elec_f1 | none | fine | 0.375 | 1.200E-06 | |
| tube2_elec_peek_f | 0.35 | fine | 0.350 | 2.306E-06 | 6.24 |
| tube2_elec_peek_f1 | 0.35 | fine | 0.375 | 1.944E-06 | 4.69 |
| | | | | | |
| tube3_elec | none | coarse | | 1.041E-05 | |
| tube3_elec_peek | 0.5 | coarse | | 1.228E-05 | 6.63 |
| tube3_elec_peek1 | 0.48 | coarse | | 1.213E-05 | 6.10 |
| tube3_elec_peek2 | 0.46 | coarse | | 1.203E-05 | 5.75 |
| tube3_elec_f | none | fine | | 1.785E-06 | |
| tube3_elec_peek_f | 0.5 | fine | | 3.521E-06 | 6.16 |
| tube3_elec_peek_f2 | 0.46 | fine | | 3.393E-06 | 5.70 |

Table 4. Simulation results without and with a PEEK fiber in a small section of the electrode gap.

Up to this point we've assumed that the electric field in the gap is independent of z, the coordinate axis along the electrode axis. We now turn to the end effects which were also determined by simulation using another feature of the same software. Here we used cylindrical symmetry to again reduce the problem to two dimensions. Figure 6 shows the upper half of a cross section of one end of an electrode. The z-axis lies along the bottom of the figure. A Neumann boundary condition was assumed at the boundary where the tube meets the left edge of the defined space (3.0 mm in from the end) so that equipotential lines will continue across this artifical boundary with the same density as on the side within the boundary. The right boundary opposite the open end of the electrode is held at ground. This distorts the fringe field a bit but it appears to have a very small effect on the answer. In this case of cylindrical symmetry the integral of the energy density is in units of Joules since the volume is known. Again we calculated the difference in capacitance with and without the end. For the case without an end we simulated a very long electrode and took just the central 6 mm length. The simulation agreed exactly with hand calculations of this simple case. Table 5 shows the results. Because the length of the electrode end section was 3 mm long and the length of the

electrode section far from the end was 6 mm long, we took half the energy of the 6 mm section to subtract from the energy in the electrode end section. The results in Table 4 are for one end while the results carried over to Table 3 include both ends of the electrode.

| File | Geometry | Energy (J) | Change in Capacitance (pF) |
|---|---|---|---|
| tube1_end | As described in text | 5.394E-08 | 0.182 |
| tube1_end1 | 6 mm of middle of electrode | 9.650E-08 | |
| tube2_end | As described in text | 1.011E-07 | 0.181 |
| tube2_end1 | 6 mm of middle of electrode | 1.768E-07 | |
| tube3_end | As described in text | 1.493E-07 | 0.196 |
| tube3_end1 | 6 mm of middle of electrode | 2.498E-07 | |
| tube3_end2 | Electrode in matrix | 1.495E-07 | 0.002 |
| tube3_end3 | Tube length 1 mm longer than rod | 1.537E-07 | 0.035 |

Table 5. Simulation results at and away from the electrode ends. The difference, suitably normalized, gives the contribution to the electrode capacitance due to end effects.

| | FCal1 | | FCal2 | | FCal3 | |
|---|---|---|---|---|---|---|
| Tube ID | 5.249 mm | | 5.63 mm | | 3.25 mm | |
| Rod OD | 4.712 mm | | 4.93 mm | | 2.75 mm | |
| Rod Length | 0.4452 mm | | 0.4434 m | | 0.4434 m | |
| Potential | 250 V | | 375 V | | 500 V | |
| Offset (mm) | Energy Density (J/m) | Capacitance (pF) | Energy Density (J/m) | Capacitance (pF) | Energy Density (J/m) | Capacitance (pF) |
| 0.000 | 8.054E+06 | 229 | 1.473E-05 | 186 | 2.081E-05 | 148 |
| 0.025 | 8.089E-06 | 230 | 1.477E-05 | 186 | 2.084E-05 | 148 |
| 0.050 | 8.197E-06 | 234 | 1.488E-05 | 188 | 2.092E-05 | 148 |
| 0.075 | 8.388E-06 | 239 | 1.508E-05 | 190 | 2.105E-05 | 149 |
| 0.100 | 8.678E-06 | 247 | 1.537E-05 | 194 | 2.124E-05 | 151 |
| 0.150 | 9.709E-06 | 277 | 1.630E-05 | 206 | 2.182E-05 | 155 |
| 0.200 | | | 1.795E-05 | 226 | 2.273E-05 | 161 |

Table 6. Electrode capacitance when the rod is off-centered within the tube.

The simulation included just an electrode. But the electrodes are embedded in a matrix which would modify the field lines in the upper part of Figure 6. So we increased the

tube wall thickness to simulate the effect of the matrix. The difference between an electrode in the matrix and an isolated electrode is only 2 fF (at one end) so we neglected it. We also simulated the case that the rod is shorter than the tube by 2 mm (1 mm at each end). This is more than a factor two larger than the length differences shown in Table 1. Again this small effect was neglected.

Finally we used the simulation program to calculate the electrode capacitance in the case that the rod was offset within the tube. Table 6 shows the electrode component dimensions chosen for this study. Here the capacitance does not include the PEEK insulating fiber and the end effects. Note that the capacitance increases with larger offsets. The increase is very small for smaller offsets. Offsets of more than about 0.025 to 0.050 mm seem unreasonable.

The measurements summarized here represent a large effort by members of the FCal community. By measuring the capacitance of 12,260 electrodes in each of the two FCal1 modules, 10,200 electrodes in each of the two FCal2 modules, and 8,224 electrodes in each of the two FCal3 modules we found electrode-to-electrode gap uniformity at the level of 0.8%, 1.5%, and 1.2% rms respectively for the three modules. The geometrical tolerance in the gap, deduced from these measurements, makes a negligible contribution to the constant term in the energy resolution. The measured electrode capacitances agree with calculations using the geometrical measurements of the electrode components at the 2 to 3 pF level.

References

* Corresponding author.

[1] Igor Koruga, “Preliminary QC Analysis of ATLAS FCal1 Module Tubes and Rods”, October 1999/January 2000; Joshua Ruder and Charissa Fuhrmann, “Preliminary QC Tolerance Analysis of ATLAS FCal1 Module, Second Rod Shipment”, May 2002.

[2] M.Khakzad EMail of 3 Sep 2002.
P.Krieger EMail of 19 Dec 2002.
P.Krieger EMail of 22 Jan 2003.
Vance Strickland and Philippe Gravelle EMail of 24 Jan 2003
P.Krieger EMail of 24 Jan 2003.
P.Krieger EMail of 5 Feb 2003.
P.Krieger EMail of 4 Dec 2003
File capcalcsum.txt by J.Rutherfoord of 31 Oct 2003

[3] M.Khakzad EMails of 26 Aug 2002)

[4] See G.Oakham EMail of 20 Aug 2002. Also see www.sdplastics.com/peek.html